Journal of Medicinal Chemistry

Brief Article

Design, Synthesis and Biological Evaluation of Substituted Pyrimidines as Potential Phosphatidylinositol 3-Kinase (PI3K) Inhibitors

Ji-Quan Zhang, Yong-Jie Luo, Yan-Shi Xiong, Yang Yu, Zheng-Chao Tu, Zi-Jie Long, Xiao-Ju Lai, Hui-Xuan Chen, Yu Luo, Jiang Weng, and Gui Lu

J. Med. Chem., **Just Accepted Manuscript** • DOI: 10.1021/acs.jmedchem.6b00235 • Publication Date (Web): 18 Jul 2016

ACS Publications

Journal of Medicinal Chemistry is published by the American Chemical Society. 1155 Sixteenth Street N.W., Washington, DC 20036

Design, Synthesis and Biological Evaluation of Substituted Pyrimidines as Potential Phosphatidylinositol 3-Kinase (PI3K) Inhibitors

Ji-Quan Zhang,[†,‡] Yong-Jie Luo,[†] Yan-Shi Xiong,[†] Yang Yu,[†] Zheng-Chao Tu,[§] Zi-Jie Long,[‖] Xiao-Ju Lai,[⊥] Hui-Xuan Chen,[†] Yu Luo,[†] Jiang Weng,[†] Gui Lu[*,†,#]

[†]Institute of Medicinal Chemsitry, School of Pharmaceutical Sciences, Sun Yat-sen University, Guangzhou, 510006, PR China
[‡]College of Pharmacy, Guizhou Medical University, Guiyang, 550004, PR China
[§]Guangzhou Institute of Biomedicine and Health, Chinese Academy of Sciences, Guangzhou, 510530, PR China
[‖]Department of Hematology, The Third Affiliated Hospital, Sun Yat-sen University, Guangzhou, 510260, PR China
[⊥]State Key Laboratory of Oncology in South China, Cancer Center, Sun Yat-sen University, Guangzhou, 510060, PR China
[#]Institute of Human Virology, Sun Yat-sen University, Guangzhou, 510080, PR China

KEYWORDS: Substituted pyrimidine, PI3Kα, isozyme selectivity, cytotoxicity

ABSTRACT: Three series of substituted pyrimidines were designed and synthesized. All target compounds were screened for kinase inhibitory activities against PI3Kα, and most IC_{50} values were found within the nanomolar range. Compounds **5d** and **5p** displayed comparable activities relative to the positive control **5a**, **5p** also showed a significant isozyme selectivity (PI3Kβ/α). Furthermore, the cytotoxicities of these pyrimidines against human cancer cell lines were evaluated, the *in vivo* anticancer effect of **5d** was also tested.

INTRODUCTION

It is well recognized that phosphatidylinositol 3-kinases (PI 3-kinases or PI3Ks) play a central role in a broad cellular functions such as cell growth, proliferation, differentiation, survival, and intracellular trafficking.[1,2] On the basis of sequence homology and substrate preferences, PI3Ks can be categorized into class I, II, and III.[3] Class I PI3Ks are further subdivided into class IA and class IB. Class IA PI3Ks (PI3Kα, PI3Kβ, and PI3Kδ) consist of heterodimers between a p110 catalytic subunit (p110α, p110β, and p110δ, respectively) and a p85 regulatory subunit. The Class IB subtype (PI3Kγ) contains a catalytic p110γ and a regulatory p101 subunit.[4] The main function of class I PI3Ks *in vivo* is to phosphorylated phosphatidylinositol (4,5) diphosphate (PtdIns(4,5)P2, PIP2) to phosphatidylinositol triphosphate (3,4,5)P3 (PIP3) at the 3-position of the inositol ring, which serves as an important second messenger in triggering a series of downstream effectors mediating cellular functions. This process is strictly controlled by tumor suppressor phosphatase and tensin homologue (PTEN), which dephosphorylates PIP3 back to PIP2.[5] Abnormalities in functions of both kinase and phosphatase are commonly observed in tumors, thus emphasizing the importance of this pathway in cancer. A high proportion of human cancers were revealed to rely strongly on P110α for survival and resistance to therapy.[5,6] Therefore, the targeting of PI3K pathway is one of the most promising approaches for cancer treatment.

Among the current clinical candidates (Figure 2), **NVP-BKM120**, a pyrimidine scaffold derivative developed by Novartis AG, displayed a potent and selective class I PI3K inhibitor over many other related kinases;[7] this derivative is also undergoing phase III trials for breast cancer treatment (NCT01572727, NCT01610284, and NCT01633060). Similar to the majority of reported clinical candidates, **NVP-BKM120** showed comparable potency against four isoforms of class I PI3Ks, possibly leading to off-target effects compromising therapeutic utility. Therefore, more potent and higher isoform-selective chemical entities should be developed in clinical trials to offer a better choice for cancer treatment. On the basis of 2,4,6-trisubstituted pyrimidine derivatives, most previous structure-activity relationships (SAR) studies focused on the 4- and 6-positions of the pyrimidine scaffold with morpholine substituted on the 2-position.[7,8] This finding led us to design and synthesize a series of derivatives by replacing the C_2 morpholine with various aliphatic or long-chain substituted aromatic amines. Increased hydrogen bonding on the periphery of the active site was expected to improve selective profiles (Figure 3), leading to the identification of compounds **5d** and **5p**.

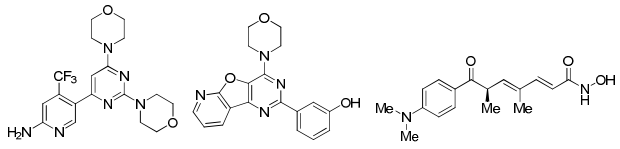

Figure 1. Structures of positive controls mentioned in this study.

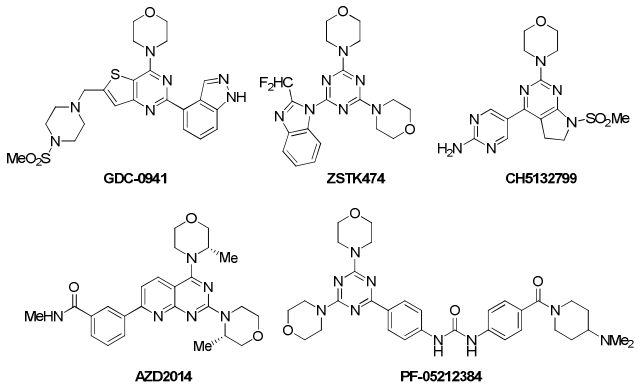

Figure 2. Some reported structures of clinical candidates.

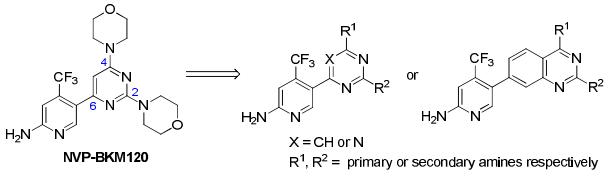

Figure 3. Design of series derivatives based on **NVP-BKM120.**

RESULTS AND DISCUSSION

As outlined in Scheme 1, the desired 2,4,6-trisubstituted pyrimidine derivatives (**5a-p**) were prepared from 2,4,6-trichloropyrimidine (**1**) via amination on C_4 and C_2 stepwise with various aliphatic amines or aromatic amines. Suzuki-Miyaura cross-coupling reaction with 5-(4,4,5,5-tetramethyl-1,3,2-dioxaborolan-2-yl)-4-(trifluoromethyl)pyridin-2-amine (**4**) was then performed under microwave irradiation conditions. Optically pure compounds **6** and **7** were obtained from **5d** via chiral preparative separation (Figure 4). The 2,4,6-trisubstituted-1,3,5-triazines (**11a-e**) were prepared through a similar procedure mentioned above (Scheme 2). Compounds **12** and **13** were also isolated from **11b** via chiral separation (Figure 5).

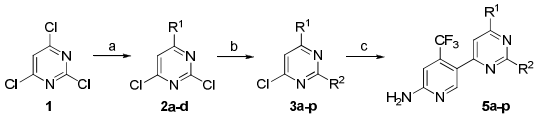

Scheme 1.

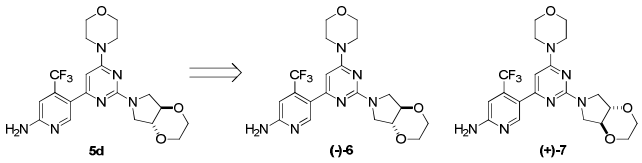

Figure 4. Structures of compounds **6** and **7**.

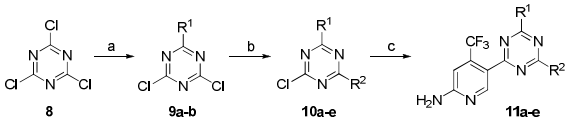

Scheme 2.

Scheme 3 shows the detailed synthetic route for the preparation of quinazoline-scaffold derivatives **18a** and **18b**. Starting with 2-amino-4-chlorobenzoic acid (**14**), intermediate **15** was obtained via cyclization with urea, which was subjected to chlorination with $POCl_3$ in a basic environment to obtain the key intermediate **16**. Coupling with morpholine and (2*S*,6*R*)-2,6-dimethylmorpholine was then performed to produce **17a** and **17b**, respectively, which underwent Suzuki-Miyaura cross-coupling reaction with **4** to generate the target compounds. The 6-pyrimidine-substituted derivative **20** was prepared from **3d** and boronic ester **20** via a similar coupling reaction (Scheme 4).

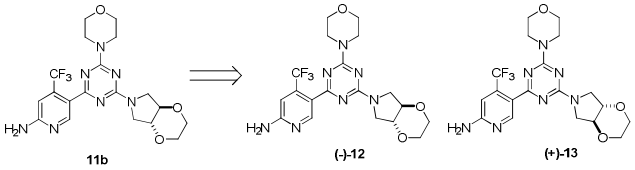

Figure 5. Structures of compounds**12** and **13**

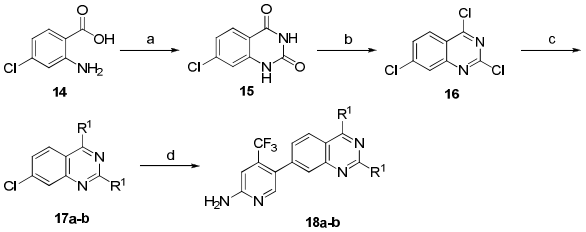

Scheme 3.

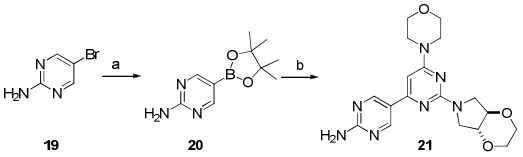

Scheme 4.

The detailed preparation of *trans*-hexahydro-*2H*-[1,4]dioxino[2,3-c]pyrrole (**26**) is shown in Scheme 5. Starting with benzyl 2,5-dihydro-*1H*-pyrrole-1-carboxylate (**22**), intermediate **25** was obtained via epoxidation with *m*-CPBA, nucleophilic substitution with 2-bromoethanol in the presence of $BF_3{\cdot}OEt_2$, and subsequent cyclization in EtOH. Removal of the protecting group with 10% Pd/C produced the desired intermediate **26**.

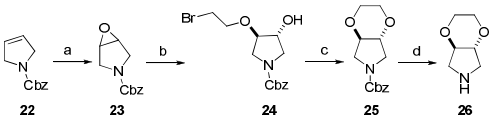

Scheme 5.

All newly prepared compounds were assessed *in vitro* in terms of biological activity against the p110α isoform of PI3K by using the kinase-Glo Plus Luminescent Assay. **PI-103** and **NVP-BKM120** (**5a**) were assigned as positive controls. Under these assay conditions, IC_{50} values were determined to be 7.4±1.3 nM and 28.0±1.2 nM, respectively (Table 1).

We first conducted an SAR study by replacing the C_4 morpholine with 2,6-dimethylmorpholine and hexahydro-*2H*-[1,4]dioxino[2,3-c]pyrrole. All tested compounds (**5i-5m**) showed significant decrease in activity possibly because of increased steric hindrance, which obstructed the hydrogen bond interaction between O (morpholine) and NH (hinge Val882).[9,10] Compounds **5b-5f** were characterized by replacing

Table 1. Kinase inhibition against PI3Kα (IC_{50} values in nM).

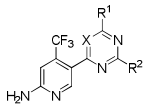

Compound	X=	R^1	R^2	IC_{50}[a]
5a	CH			28.0±1.2
5b	CH		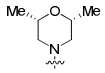	91.0±12.6
5c	CH			60.0±2.2
(±)-5d	CH			31.0±6.0
5e	CH			117.0±2.9
5f	CH		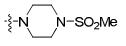	23.0±4.7
5g	CH		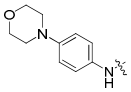	26.0±2.7
5h	CH		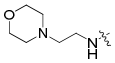	568.0±28.9
5i	CH	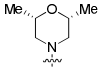		224.0±6.4
5j	CH	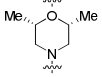	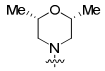	>10000
5k	CH	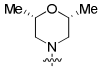		5751±1275
5l	CH			896.0±56.7
(±)-5m	CH			375.0±9.9
5n	CH		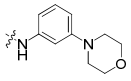	118.0±5.6
5o	CH		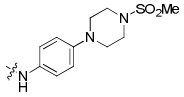	31.0±3.1

Compound	X=	R^1	R^2	IC_{50}[a]
5p	CH		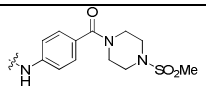	18.0±1.9
11a	N			59.0±4.5
(±)-11b	N			32.0±2.4
11c	N	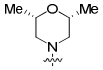		9530±1675
11d	N	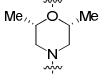		>10000
11e	N			>10000
(-)-6	CH			61.0±5.4
(+)-7	CH			35.0±2.3
(-)-12	N			68.0±8.2
(+)-13	N			38.0±4.5
(±)-21				128.0±9.1
18a				>10000
18b				>10000
PI-103				7.4±1.3

[a]*In vitro* lipid kinase assay. IC_{50} values are the mean of triplicate measurements.

the C_2 morpholine of **5a** with various heterocycles, and racemic **5d** showed comparable activity relative to reference **5a**. By contrast, *cis*-form heterocycle substituted compound **5e** exhibited a four-fold decrease in activity relative to **5d**. To further investigate the influence of chiral configuration of **5d** on the inhibitory activity, compounds **6** and **7**, which were separated from **5d**, were evaluated. Dextroisomer **7** showed approximately two-fold higher activity than levoisomer **6**.

Upon introducing an aliphatic or aromatic chain between the pyrimidine scaffold and C_2 morpholine, compound **5g** was found to be slightly more potent than **5a**. By contrast, compound **5h** showed significant loss in activity possibly because of π-π (T-shaped) stacking interaction between the benzene ring of **5g** and hinge residue of Trp780. Long-chain substituted compound **5p** displayed the highest inhibitory activity, which was 1.56 times higher than that of **5a**. We could also deduce that the pyrimidine scaffold carried a N atom at position 5 (**11a-e**, **12** and **13**), but no activity was observed upon replacing the pyrimidine scaffold with quinazoline (**18a** and **18b**).

We compared the biochemical activities of compounds **5a**, **5d** and **5p** with other isoforms of PI3Ks. As summarized in Table 2, compound **5d** showed comparable activities with **5a** to other PI3K isoforms, whereas compound **5p** showed better selectivity over β-isozyme, with a selectivity of 112-fold (PI3Kβ/α) relative to 9.3-fold of **5a**. Interestingly, **5p** also displayed an IC_{50} value of 13.0±0.5 nM against δ-isozyme, making it a promising dual PI3Kα/δ inhibitor.

Mutations of class I PI3Ks frequently occur in various human cancers;[11-13] thus, 19 human cancer cell lines were used in the current experiment, Trichostatin A (TSA) and **5a** were

Table 2. Activities of **5a**, **5d** and **5p** against class I PI3K (IC_{50} values[a] in nM).

Compound	PI3Kα	PI3Kβ	PI3Kγ	PI3Kδ
5a	28.0±1.2	259.0±13.8	129.0±9.6	62.0±7.6
5d	31.0±6.0	175.0±2.4	158.0±14.1	61.0±7.2
5p	18.0±1.9	2014.0±126.9	80.0±7.0	13.0±0.5

[a] IC_{50} values are the mean of triplicate measurements.

employed as positive controls. The results are presented in Tables 3 and 4. All tested compounds showed comparable cytotoxicities with IC_{50} values in the micromolar range, except for compounds **5l** and **18a**. Compound **5d** also exhibited comparable activities to **5a** in various cell lines, and dextroisomer **7** was twice to thrice more potent than levoisomer **6**. These results were correlated with their effects on kinase. Compound **5g** unexpectedly performed well on kinase but exhibited weak cellular inhibition.

As shown in Figure 6, the suppressive effect of compound **5d** on p-AKT^{473} was comparable to that of **5a**, whereas **5p** showed more potent inhibition. Compounds **5d** and **5p** were also shown to inhibit the PI3K/AKT/m-TOR pathway; thus, **5d** and **5p** were potential PI3K inhibitors.

We have compared the effects of compounds **5a**, **5d** and **5p** on MDA-MB-231 cell proliferation test.[14-16] The results revealed that **5a** (positive control) and **5d** showed similar anticancer effects, **5d** was more potent than **5p** (Figure 7). So we used a xenograft model to evaluate the *in vivo* anticancer effects of **5d**.

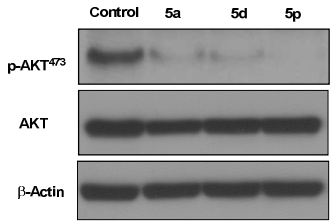

Figure 6. Effects of compounds **5a**, **5d** and **5p** on AKT and p-AKT^{473}.

Nude mice bearing MDA-MB-231 xenograft tumors were treated with **5d** (30 mg/kg, every two days) by intragastric administration for 19 days. As shown in Figures 8a and 8b, the tumor size in the **5d**-treated group (402±184 mm^3; P<0.001) was smaller than that in the control group (1065±142 mm^3), indicating that the growth of xenograft tumors was significantly inhibited by **5d**. Consistently, the tumor weight in the **5d**-treated group (0.32±0.19 g; P<0.01) was significantly lower than that in the control group (0.74±0.10 g; Figure 8c). During the experimental period, the mice in the **5d**-treated group showed no decrease in body weight (Figure 8d), indicating the low toxicity of intragastrically administered **5d**.

To examine the possible binding modes for compound **5d**, **5p** and **18a** inside the ATP-binding site of PI3Ks, docking

Table 3. Anti-proliferative activities in various cell types (IC_{50} values[a] in μM).

Cell-lines	5a	(±)-5d	5c	5b	11a	5e	5l	(±)-5m	(±)-11b	TSA
K562	1.10±0.30	4.26±1.41	2.40±0.49	2.68±0.10	>10	1.75±0.98	>10	3.19±0.76	>10	0.12±0.03
MOLT-4	0.80±0.19	1.00±0.13	1.14±0.11	0.42±0.05	1.55±0.36	2.51±0.22	NT	3.24±0.08	1.21±0.19	0.02±0.00
BEL-402	1.92±0.43	3.37±0.55	2.79±1.45	1.64±0.36	5.90±0.48	5.82±1.23	NT	6.43±1.23	5.90±1.87	0.10±0.01
Huh-7	1.51±0.29	4.26±0.21	2.93±0.30	1.21±0.22	5.67±0.79	4.84±1.18	NT	6.29±0.84	5.66±0.85	0.06±0.00
MCF-7	1.50±0.29	2.42±0.56	2.54±0.55	1.41±0.37	5.37±1.80	4.95±1.45	NT	7.29±1.41	8.15±1.34	0.07±0.01
SK-BR-3	NT	NT	NT	NT	NT	NT	NT	NT	NT	0.05±0.04
DU145	0.91±0.25	1.93±0.31	2.38±0.20	1.41±0.13	3.43±1.17	4.81±1.27	>10	7.11±0.98	3.30±0.60	0.06±0.00
U937	0.58±0.09	0.77±0.05	0.72±0.12	0.57±0.12	2.93±0.08	1.76±0.12	NT	2.86±0.65	3.05±0.14	0.04±0.00
NCI-N87	0.66±0.27	1.36±0.39	1.41±0.37	0.52±0.25	1.20±0.52	1.97±0.62	NT	6.21±1.00	0.77±0.18	0.06±0.00
SGC-901	1.24±0.27	3.14±0.14	2.30±0.12	1.24±0.04	5.25±0.95	3.75±1.52	NT	4.78±0.68	4.46±0.98	0.03±0.00
BGC-823	1.43±0.46	3.09±0.62	2.44±0.50	1.41±0.12	>10	4.57±1.43	NT	4.33±1.10	9.57±1.18	0.07±0.00
HT1080	2.08±0.35	4.73±1.00	2.72±0.84	1.98±0.88	5.51±0.02	4.84±0.11	NT	5.64±1.49	10.00±1.20	0.08±0.00
A431	1.03±0.47	3.68±1.37	1.79±0.60	2.29±0.29	8.40±2.50	2.55±1.60	NT	3.03±0.18	>10	0.18±0.03
A549	1.51±0.17	3.39±1.06	3.05±1.80	1.89±0.91	6.37±0.90	4.98±0.32	NT	5.56±1.07	4.03±0.99	0.05±0.01
PANC-1	1.83±0.66	3.26±1.32	2.78±0.39	1.38±0.28	6.42±0.63	3.67±1.41	NT	5.97±1.63	6.23±1.91	0.10±0.01
Hela	1.17±0.36	2.66±0.77	1.76±0.21	1.81±0.83	8.33±0.85	4.31±1.40	NT	5.33±1.60	>10	0.09±0.01

[a] IC_{50}, the mean value of triplicate measurements. [b] NT, not tested.

Table 4. Anti-proliferative activities in various cell types (IC_{50} values[a] in μM).

Cell-lines	5f	5g	5n	5o	5p	(-)-6	(+)-7	(-)-12	(+)-13	TSA
K562	3.64±0.56	8.81±2.10	14.90±1.82	11.20±0.86	NT[b]	6.34±0.85	2.56±0.43	24.60±1.50	24.50±3.41	0.12±0.02
HL60	NT	NT	4.34±1.51	0.94±0.20	2.49±1.22	NT	NT	2.70±0.76	4.85±1.31	NT
MOLT-4	1.11±0.22	1.77±0.52	4.07±0.85	1.11±0.20	1.96±0.50	1.96±0.35	0.97±0.44	2.28±0.24	2.08±0.03	0.02±0.00
MCF-7	4.39±1.10	9.41±0.83	16.50±2.54	4.97±1.30	12.8±2.90	7.47±1.04	3.82±0.77	7.32±1.50	9.29±2.06	0.07±0.00
SK-BR-3	1.59±0.17	2.67±1.28	6.53±1.10	1.63±0.53	4.79±0.31	3.47±0.50	1.60±0.40	4.27±1.38	3.67±0.32	0.05±0.00
MDA-MB-231	NT	NT	7.28±2.64	5.36±1.36	4.34±0.85	NT	NT	15.10±1.72	11.90±1.87	NT
DU145	6.56±1.21	>10	0.99±0.12	6.71±1.12	NT	15.03±3.47	4.86±0.045	7.36±0.98	1.08±0.12	0.05±0.01
PC3	NT	NT	2.21±0.37	7.49±1.24	19.50±0.08	NT	NT	5.63±0.83	6.24±1.95	NT
NCI-N87	NT	NT	4.66±0.47	1.29±0.22	4.22±1.05	NT	NT	3.90±0.30	2.77±0.46	0.05±0.01
U937	1.99±0.26	3.48±0.86	10.40±3.53	2.39±1.04	4.74±1.35	3.38±0.72	1.51±0.50	4.03±0.45	5.53±0.46	0.04±0.00
BGC-823	3.64±1.00	8.36±0.74	NT	NT	NT	6.59±0.50	2.79±1.20	NT	NT	0.06±0.01
A431	NT	NT	11.50±1.47	5.90±0.87	10.50±2.11	NT	NT	14.10±0.78	32.20±5.21	0.18±0.02
A549	2.95±0.35	7.79±1.48	4.57±0.96	5.46±0.05	9.13±0.78	6.40±2.01	2.49±0.36	8.01±0.48	9.50±1.90	0.05±0.01
PANC-1	NT	NT	8.52±1.37	2.36±0.09	3.47±0.49	NT	NT	9.04±2.50	7.64±1.05	0.10±0.01
Hela	4.04±1.90	6.91±1.55	>100	>100	>100	7.53±1.48	2.45±0.33	>100	>100	0.09±0.03

[a] IC_{50}, the mean value of triplicate measurements. [b] NT, not tested.

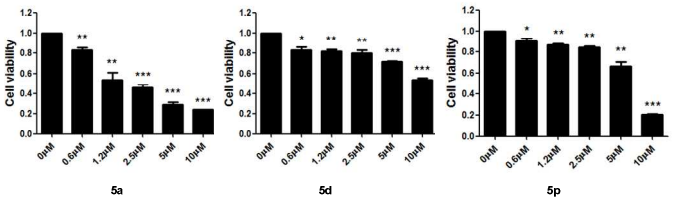

Figure 7. Effects of compounds **5a**, **5d** and **5p** on cell proliferation test.

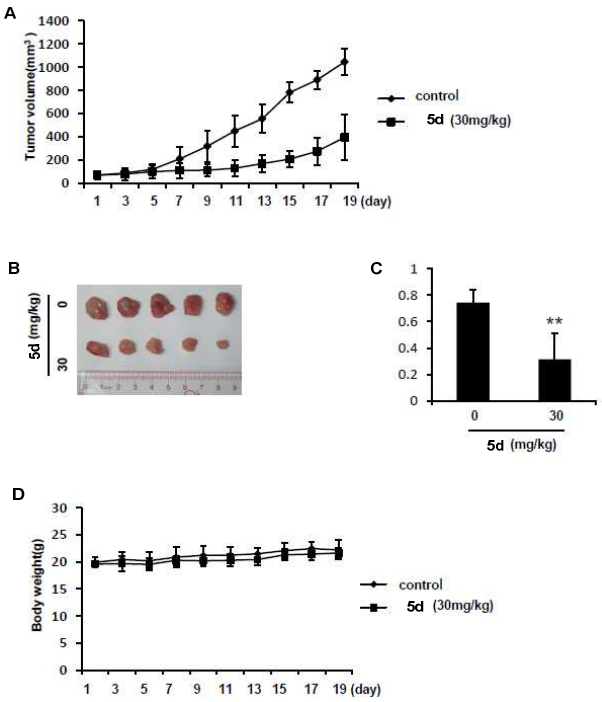

Figure 8. 5d attenuates xenograft tumor growth. (a) Nude mice bearing MDA-MB-231xenograft tumors were treated with vehicle or **5d** (30 mg/kg, intragastric administration, every two days). The estimated tumor volume is plotted versus time. (b) Tumors were removed from 5 mice in each group and are shown. (c) The weights of the dissected tumors were measured. (d) The body weights were monitored and plotted versus time. All data are presented as the mean±SD (n =5; **, P < 0.01, ***, P < 0.001, Student t test).

analysis was performed using C-DOCKER in Discovery Studio 2.5. The protein crystal structure of PI3Kα (PDB code, 3ZIM)[17] was used, followed by 8-ns molecular dynamics simulations to study the binding modes using the Amber12 package. Three hydrogen bonds interacted between **5d** and PI3Kα (Figure 9a): the oxygen of C_4 morpholine formed a key hydrogen bond with the hinge of Val851 (distance: 1.9 Å), and the amino of the pyridine ring formed two hydrogen bonds, which interacted with the side chains of residues Asp993 (distance: 2.0 Å) and Lys802 (distance: 2.1 Å). Compound **5p** also exhibited the above mentioned three-hydrogen-bond interaction, although it indicated additional π-π (T-shaped) stacking interaction between the benzene ring and hinge residue of Trp780 (Figure 10a). This finding led to a more potent activity against PI3Kα than **5d**. The docking analysis of **5p** with PI3Kβ (PDB code, 3T8M) (Figure 10b) showed that this compound formed a hydrogen bond with a residue of Val882 (distance: 1.9 Å) and a π-π (T-shaped) stacking interaction with residue Trp812. Surprisingly, the amino of the pyridine ring only formed a hydrogen bond with residue Asp964 (distance: 2.2 Å), and no interaction existed with residue Lys833, which may explain its good selectivity over PI3Kβ. We also performed the docking analysis of compound **5p** binding to γ (PDB code, 4ANV) (Figure 10c) and δ isoforms (PDB code, 2WXF) (Figure 10d). Four hydrogen-bond interactions with residues of PI3Kγ were noticed: Val882 (1.8 Å), Tyr867 (2.1 Å), Asp841 (2.1 Å), and Gln893 (2.3 Å). For the binding of compound **5p** to PI3Kδ, six hydrogen-bond interactions with the residues were indicated: Val828 (2.0 Å), Tyr813 (1.8 Å), Asp787 (1.9 Å), Lys779 (1.8 Å), Lys708 (2.1Å), and Thr750 (2.1 Å), along with a π-π (T-shaped) stacking interaction with residue Trp760. Compound **18a** expectedly showed no hydrogen-bond interaction with amino because of the replacement of pyrimidine scaffold with quinazoline, which blocked the molecule from docking into an active pocket (Figure 9b).

CONCLUSIONS

We have designed and synthesized three series of trisubstituted pyrimidine derivatives. These compounds were evaluated as potential PI3Kα inhibitors. Compound **5d** showed comparable bioactivity with **NVP-BKM120**, and **5p** displayed the greatest inhibitory potency. The isozyme-selective assay showed that **5p** exhibited higher selectivity than **5a**, suggesting that **5p** is a promising dual PI3Kα/δ inhibitor. Moreover, the cytotoxicities of the substituted pyrimidines against human cancer cell lines were evaluated, most of them showed comparable activities, the *in vivo* anticancer effect of **5d** was also tested. Their pharmacokinetics profiles and other biological activities *in vivo* are presently being investigated.

EXPERIMENTAL SECTION

Molecular modeling. The PI3Kα-KKR protein-ligand complex crystal structure (PDB ID: 3ZIM) was chosen as the template to compare the docking mode among compounds **18a**, **5d** and **5p** bound to PI3Kα, as well as **5p** bound to PI3Kβ (PDB ID: 3T8M). The molecular docking procedure was per formed in accordance with the C-DOCKER protocol of Discovery Studio 2.5. For ligand preparation, the 3D structures of compounds **18a**, **5d**, and **5p** were generated and minimized using Discovery Studio 2.5. Hydrogen atoms were added for enzyme preparation, and CHARMm force field was employed. PI3Kα and PI3Kβ enzymes were defined as receptors, and the site sphere was selected on the basis of the ligand binding location of KKR. The KKR molecule was then removed, and compounds **18a**, **5d** or **5p** were placed during the molecular docking procedure. The types of interactions between the docked enzyme and the ligand were analyzed at the end of the molecular docking. The ligand-protein complex with the optimum score was selected as the initial structure for MD simulations.[18-23]

ASSOCIATED CONTENT

Supporting information

Synthetic schemes and experimental procedures, characterization of organic molecules, enzyme assays, cell proliferation assay, western blot assay, tumor growth in xenografts. This material is available free of charge via the Internet at http://pubs.acs.org."

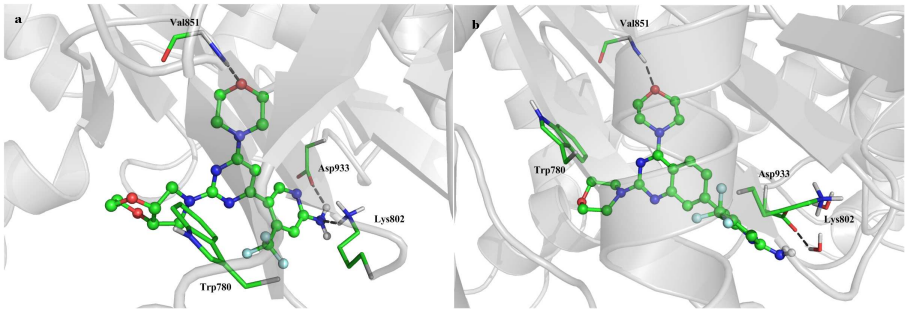

Figure 9. Docking modes for compounds **5d** and **18a** into protein crystal structure of PI3Kα. (a) Compound **5d** bound to PI3Kα. (b) Compound **18a** bound to PI3Kα (PDB ID: 3ZIM).

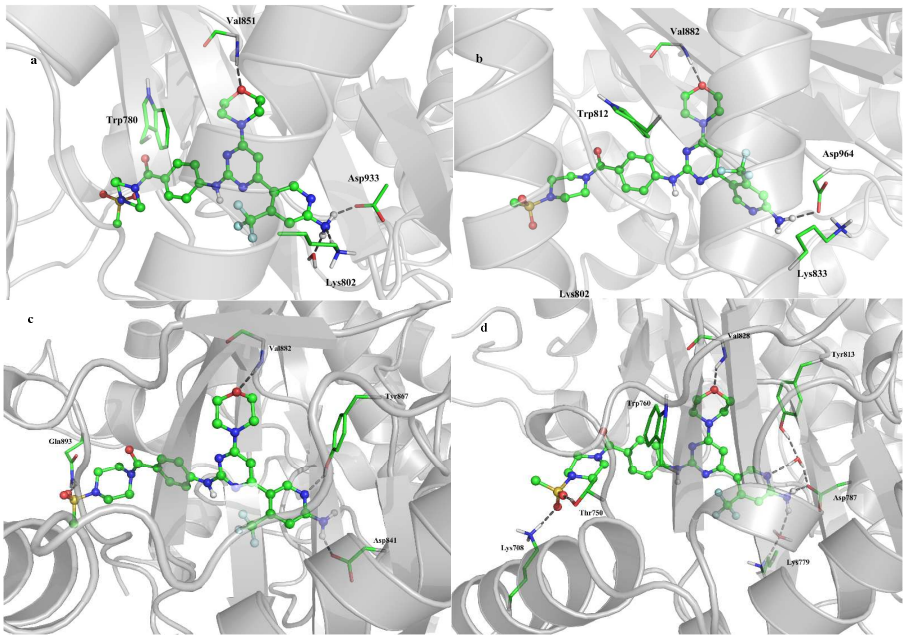

Figure 10. Docking modes for compound **5p** into protein crystal structure of PI3Ks. (a) Binding to PI3Kα (PDB ID: 3ZIM). (b) Binding to PI3Kβ (PDB ID: 3T8M). (c) Binding to PI3Kγ (PDB ID: 4ANV). (d) Binding to PI3Kδ (PDB ID: 2WXF).

AUTHOR INFORMATION

Corresponding Author

* G.Lu.: phone, 86-20-39943048; E-mail, lugui@mail.sysu.edu.cn.

Author Contributions

The manuscript was written through contributions of all authors. All authors have given approval to the final version of the manuscript.

ACKNOWLEDGMENTS

This work was financially supported by the National High-tech R&D Program of China (863 Program, No. 2013AA092903) and the Guangdong Province Natural Science Foundation (No. 2015A030313184). We also acknowledge Prof. Rui-Bo Wu for help in molecular docking.

ABBREVIATIONS LIST

PI3K, phosphatidylinositol 3-kinase; PtdIns(4,5)P2, phosphatidylinositol (4,5) diphosphate; PIP3, phosphatidylinositol triphosphate (3,4,5)P3; PTEN, phosphatase and tensin homologue; AKT, known as protein kinase B or PKB; TSA, trichostatin A; m-TOR, mammalian target of rapamycin; HEPES, 4-(2-hydroxyethyl)-1-piperazineethanesulfonic acid; EGTA, ethylene glycol tetraacetic acid; CHAPS, 3-[(3-cholamidopropyl)-dimethylammonio]-1-propane sulfonate; DMEM, dulbecco minimum essential medium; CHARMm, Chemistry at Harvard Macromolecular Mechanics; KKR, Korringa-Kohn-Rostoker; MD, molecular dynamics.

REFERENCES

(1) Vivanco, I.; Sawyers, C. L. The phosphatidylinositol 3-Kinase-AKT pathway in human cancer. *Nat. Rev. Cancer* **2002**, *2*, 489-501.

(2) Smith, A. L.; D'Angelo, N. D.; Bo, Y. Y.; Booker, S. K.; Cee, V. J.; Herberich, B.; Hong, F.-T.; Jackson, C. L. M.; Lanman, B. A.; Liu, L.; Nishimura, N.; Pettus, L. H.; Reed, A. B.; Tadesse, S.; Tamayo, N. A.; Wurz, R. P.; Yang, K.; Andrews, K. L.; Whittington, D. A.; McCarter, J. D.; Miguel, T. S.; Zalameda, L.; Jiang, J.; Subramanian, R.; Mullady, E. L.; Caenepeel, S.; Freeman, D. J.; Wang, L.; Zhang, N.; Wu, T.; Hughes, P. E.; Norman, M. H. Structure-Based Design of a Novel Series of Potent, Selective Inhibitors of the Class I Phosphatidylinositol 3-Kinases. *J. Med. Chem.* **2012**, *55*, 5188-5219.

(3) Engelman, J. A.; Luo, J.; Cantley, L. C. The evolution of phosphatidylinositol 3-kinases as regulators of growth and metabolism. *Nat. Rev. Genet.* **2006**, *7*, 606-619.
(4) Vanhaesebroeck, B.; Leevers, S. J.; Ahmadi, K.; Timms, J.; Katso, R.; Driscoll, P. C.; Woscholski, R.; Parker, P. J.; Waterfield, M. D. Synthesis and function of 3-phosphorylated insitol lipids. *Annu. Rev. Biochem.* **2001**, *70*, 535-602.
(5) Liu, P.; Cheng, H.; Roberts, T. M.; Zhao, J. J. Targeting the phosphoinositide 3-kinase pathway in cancer. *Nat. Rev. Drug Discov.* **2009**, *8*, 627-644.
(6) Hollander, M. C.; Blumenthal, G. M.; Dennis, P. A. PTEN loss in the continuum of common cancers, rare syndromes and mouse models. *Nat. Rev. Cancer* **2011**, *11*, 289-301.
(7) Burger, M. T.; Pecchi, S.; Wagman, A.; Ni, Z.-J.; Knapp, M.; Hendrickson, T.; Atallah, G.; Pfister, K.; Zhang, Y.; Bartulis, S.; Frazier, K.; Ng, S.; Smith, A.; Verhagen, J.; Haznedar, J.; Huh, K.; Iwanowicz, E.; Xin, X.; Menezes, D.; Merritt, H.; Lee, I.; Wiesmann, M.; Kaufman, S.; Crawford, K.; Chin, M.; Bussiere, D.; Shoemaker, K.; Zaror, I.; Maira, S.-M.; Voliva, C. F. Identification of NVP-BKM120 as a potent, pelective, orally bioavailable class I PI3 kinase inhibitor for treating cancer. *ACS Med. Chem. Lett.* **2011**, *2*, 774-779.
(8) Burger, M. T.; Knapp, M.; Wagman, A.; Ni, Z.-J.; Hendrickson, T.; Atallah, G.; Zhang, Y.; Frazier, K.; Verhagen, J.; Pfister, K.; Ng, S.; Smith, A.; Bartulis, S.; Merrit, H.; Weismann, M.; Xin, X.; Haznedar, J.; Voliva, C. F.; Iwanowicz, E.; Pecchi, S. Synthesis and in vitro and in vivo evaluation of phosphoinositide-3-kinase inhibitors. *ACS Med. Chem. Lett.* **2010**, *2*, 34-38.
(9) Walker, E. H.; Pacold, M. E.; Perisic, O.; Stephens, L.; Hawkins, P. T.; Wymann, M. P.; Williams, R. L. Structural determinants of phosphoinositide 3-kinase inhibition by Wortmannin, LY294002, Quercetin, Myricetin, and Staurosporine. *Mol. Cell* **2000**, *6*, 909-919.
(10) Knight, Z. A.; Chiang, G. G.; Alaimo, P. J.; Kenski, D. M.; Ho, C. B.; Coan, K.; Abraham, R. T.; Shokat, K. M. Isoform-specific phosphoinositide 3-kinase inhibitors from an arylmorpholine scaffold. *Bioorg. Med. Chem.* **2004**, *12*, 4749-4759.
(11) temke-Hale, K.; Gonzalez-Angulo, A. M.; Lluch, A.; Neve, R. M.; Kuo, W.-L.; Davies, M.; Carey, M.; Hu, Z.; Guan, Y.; Sahin, A.; Symmans, W. F.; Pusztai, L.; Nolden, L. K.; Horlings, H.; Berns, K.; Hung, M.-C.; van de Vijver, M. J.; Valero, V.; Gray, J. W.; Bernards, R.; Mills, G. B.; Hennessy, B. T. An integrative genomic and proteomic analysis of PIK3CA, PTEN, and AKT mutations in breast cancer. *Cancer Res.* **2008**, *68*, 6084-6091.
(12) Thomas, R. K.; Baker, A. C.; DeBiasi, R. M.; Winckler, W.; LaFramboise, T.; Lin, W. M.; Wang, M.; Feng, W.; Zander, T.; MacConaill, L. E.; Lee, J. C.; Nicoletti, R.; Hatton, C.; Goyette, M.; Girard, L.; Majmudar, K.; Ziaugra, L.; Wong, K.-K.; Gabriel, S.; Beroukhim, R.; Peyton, M.; Barretina, J.; Dutt, A.; Emery, C.; Greulich, H.; Shah, K.; Sasaki, H.; Gazdar, A.; Minna, J.; Armstrong, S. A.; Mellinghoff, I. K.; Hodi, F. S.; Dranoff, G.; Mischel, P. S.; Cloughesy, T. F.; Nelson, S. F.; Liau, L. M.; Mertz, K.; Rubin, M. A.; Moch, H.; Loda, M.; Catalona, W.; Fletcher, J.; Signoretti, S.; Kaye, F.; Anderson, K. C.; Demetri, G. D.; Dummer, R.; Wagner, S.; Herlyn, M.; Sellers, W. R.; Meyerson, M.; Garraway, L. A. High-throughput oncogene mutation profiling in human cancer. *Nat. Genet.* **2007**, *39*, 347-351.
(13) Samuels, Y.; Wang, Z.; Bardelli, A.; Silliman, N.; Ptak, J.; Szabo, S.; Yan, H.; Gazdar, A.; Powell, S. M.; Riggins, G. J.; Willson, J. K. V.; Markowitz, S.; Kinzler, K. W.; Vogelstein, B.; Velculescu, V. E. High frequency of mutations of the PIK3CA gene in human cancers. *Science* **2004**, *304*, 554.
(14) Kim, K. J.; Wang, L.; Su, Y.-C.; Gillespie, G. Y.; Salhotra, A.; Lal, B.; Laterra, J. Systemic anti-hepatocyte growth factor-monoclonal antibody therapy induces the regression of intracranial glioma xenografts. *Clin. Cancer Res.* **2006**, *12*, 1292-1298.
(15) Jiang, W.; Jin, G.; Ma, D.; Wang, F.; Fu, T.; Chen, X.; Chen, X.; Jia, K.; Marikar, F. M. M. T.; Hua, Z. Modification of cyclic NGR tumor neovasculature-homing motif sequence to human plasminogen kringle 5 improves inhibition of tumor growth. *PLoS ONE* **2012**, *7*, e37132.5.
(16) Zhang, F.-M.; Long, Z.-J.; Hou, Z.-J.; Luo, Y.; Xu, L.-Z.; Xia, J.-L.; Lai, X.-J.; Liu, J.-W.; Wang, X.; Kamran, M.; Yan, M.; Shao, S.-J.; Lam, E. W.-F.; Wang, S.-W.; Lu, G.; Liu, Q. A novel small molecule aurora kinase inhibitor attenuates breast tumor-initiating cells and overcomes drug resistance. *Mol. Cancer Ther.* **2014**, *13*, 1991-2003.
(17) Nacht, M.; Qiao, L.; Sheets, M. P.; St. Martin, T.; Labenski, M.; Mazdiyasni, H.; Karp, R.; Zhu, Z.; Chaturvedi, P.; Bhavsar, D.; Niu, D.; Westlin, W.; Petter, R. C.; Medikonda, A. P.; Singh, J. Discovery of a potent and isoform-selective targeted covalent inhibitor of the lipid kinase PI3Kα. *J. Med. Chem.* **2013**, *56*, 712-721.
(18) Duan, Y.; Wu, C.; Chowdhury, S.; Lee, M. C.; Xiong, G.; Zhang, W.; Yang, R.; Cieplak, P.; Luo, R.; Lee, T.; Caldwell, J.; Wang, J.; Kollman, P. A point-charge force field for molecular mechanics simulations of proteins based on condensed-phase quantum mechanical calculations. *J. Comput. Chem.* **2003**, *24*, 1999-2012.
(19) Wang, J.; Wolf, R. M.; Caldwell, J. W.; Kollman, P. A.; Case, D. A. Development and testing of a general amber force field. *J. Comput. Chem.* **2004**, *25*, 1157-1174.
(20) Bayly, C. I.; Cieplak, P.; Cornell, W.; Kollman, P. A. A well-behaved electrostatic potential based method using charge restraints for deriving atomic charges: the RESP model. *J. Phys. Chem.* **1993**, *97*, 10269-10280.
(21) Berendsen, H. J. C.; Postma, J. P. M.; van Gunsteren, W. F.; DiNola, A.; Haak, J. R. Molecular dynamics with coupling to an external bath. *J. Chem. Phys.* **1984**, *81*, 3684-3690.
(22) Jorgensen, W. L.; Chandrasekhar, J.; Madura, J. D.; Impey, R. W.; Klein, M. L. Comparison of simple potential functions for simulating liquid water. *J. Chem. Phys.* **1983**, *79*, 926-935.
(23) Ryckaert, J.-P.; Ciccotti, G.; Berendsen, H. J. C. Numerical integration of the cartesian equations of motion of a system with constraints: molecular dynamics of n-alkanes. *J. Comput. Phys.* **1977**, *23*, 327-341.

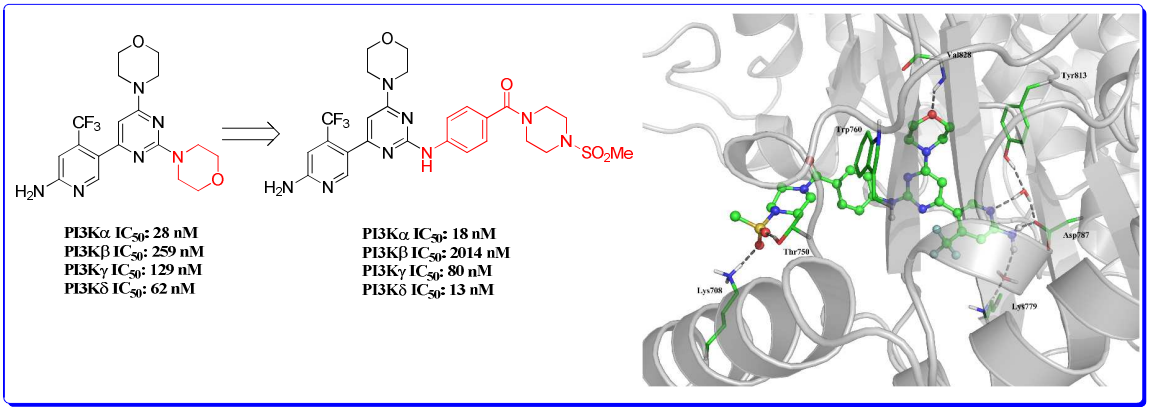
PI3Kα IC50: 28 nM
PI3Kβ IC50: 259 nM
PI3Kγ IC50: 129 nM
PI3Kδ IC50: 62 nM
PI3Kα IC50: 18 nM
PI3Kβ IC50: 2014 nM
PI3Kγ IC50: 80 nM
PI3Kδ IC50: 13 nM
Val828
Tyr813
Trp760
Asp787
Thr750
Lys708
Lys779

Figure 1.

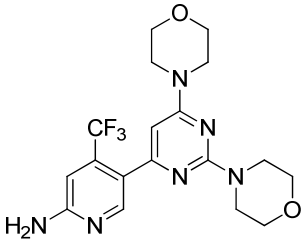

NVP-BKM120

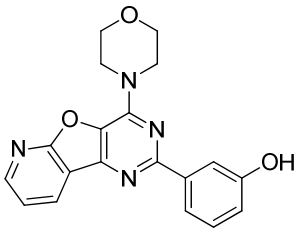

PI-103

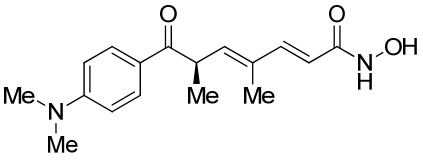

Trichostatin A

Figure 2.

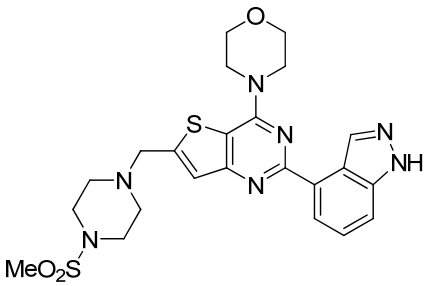

GDC-0941

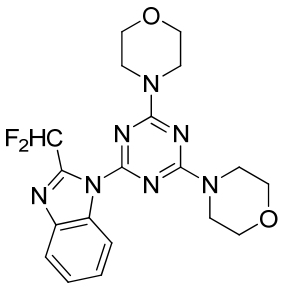

ZSTK474

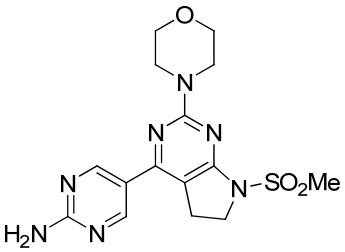

CH5132799

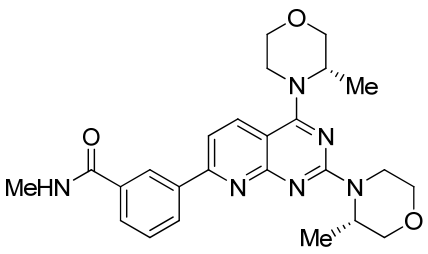

AZD2014

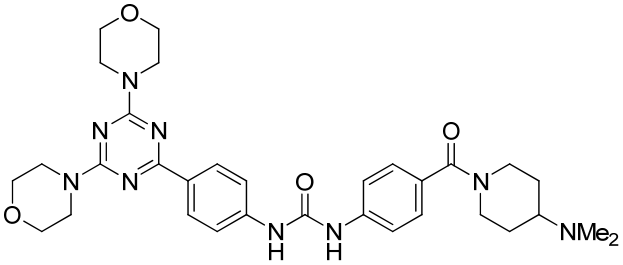

PF-05212384

Figure 3.

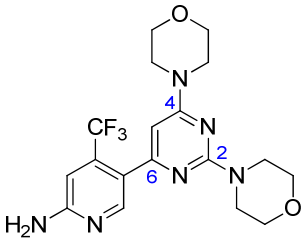

NVP-BKM120

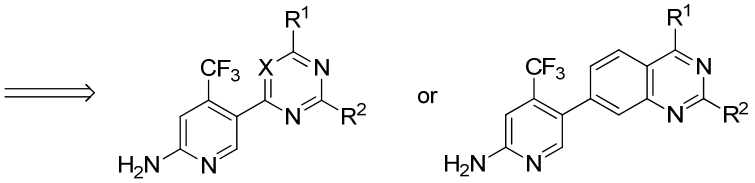

X = CH or N

R^1, R^2 = primary or secondary amines respectively

Figure 4.

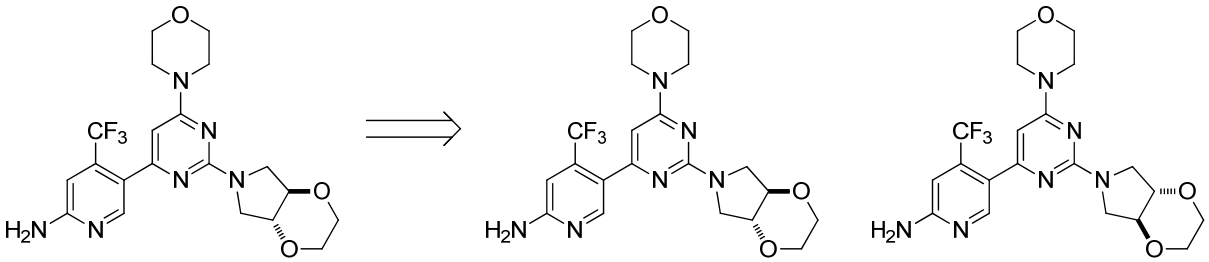

Figure 5.

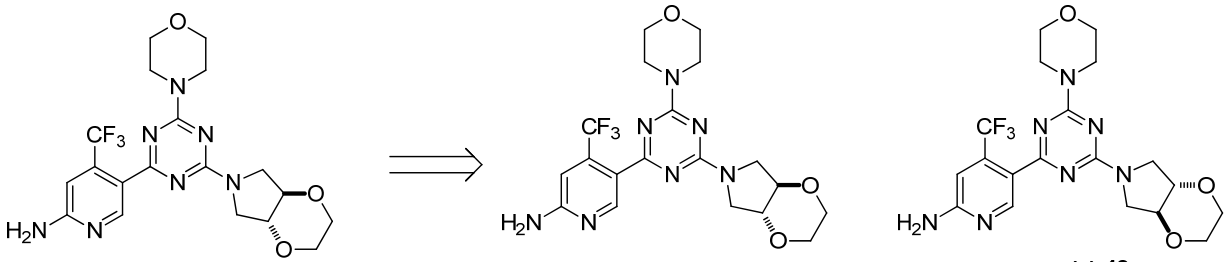

Figure 6.

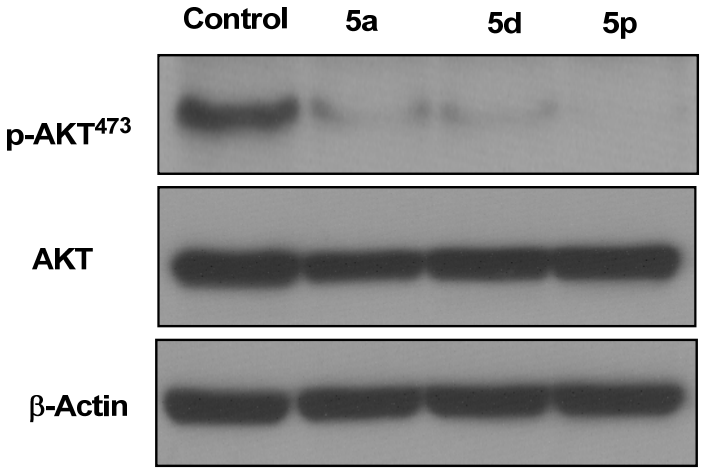

Figure 7.

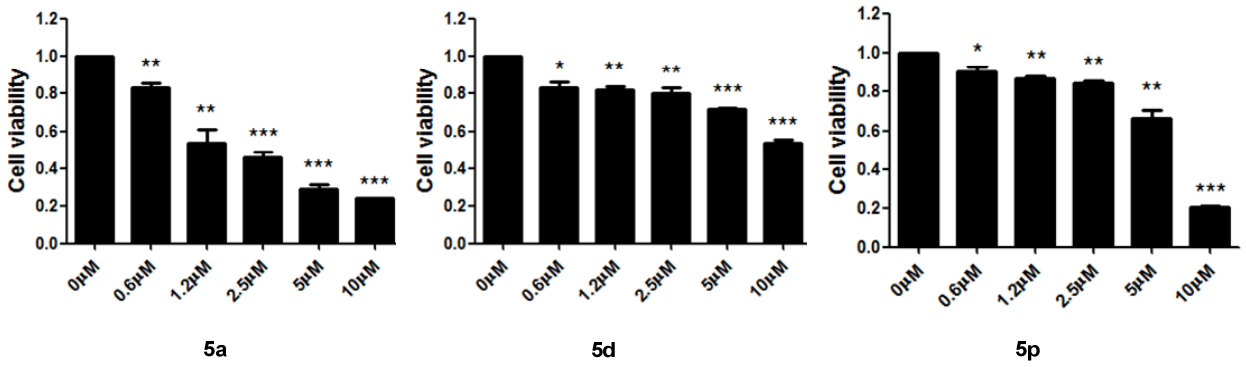

Figure 8.

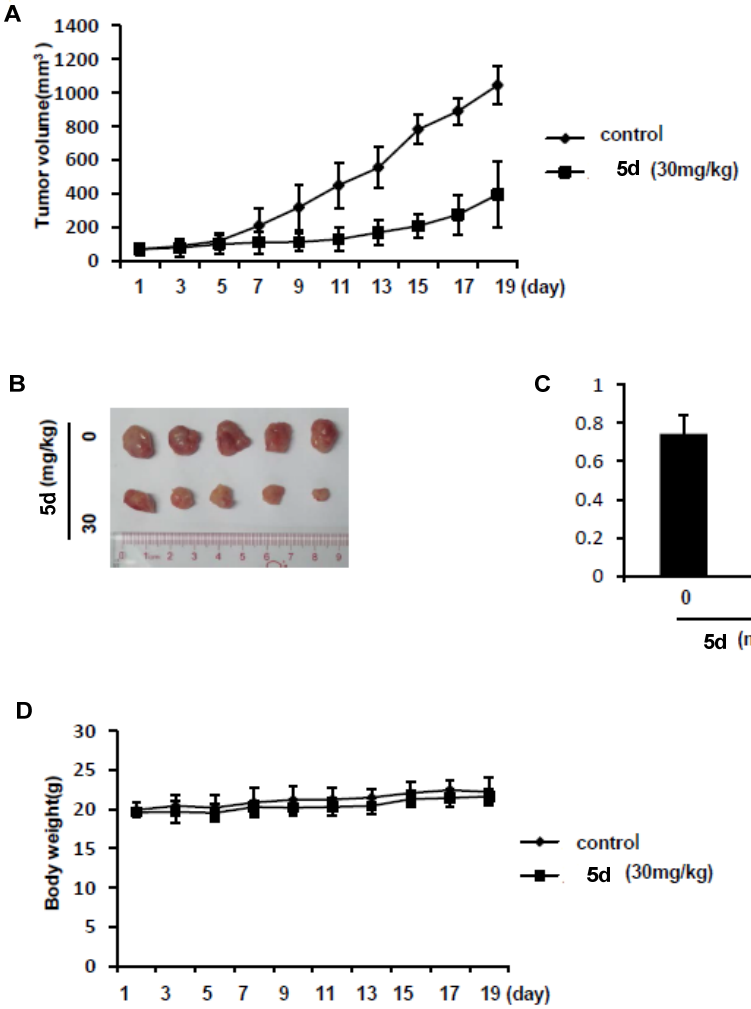

Figure 9.

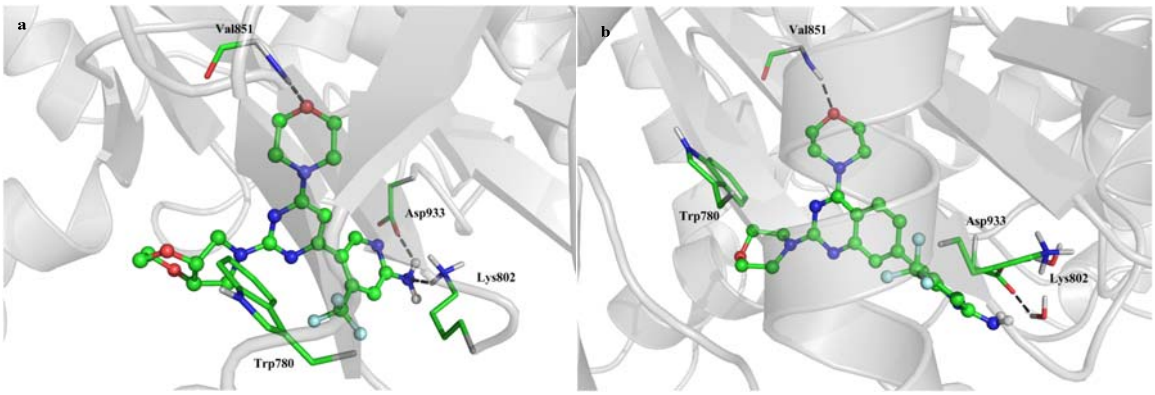

Figure 10.

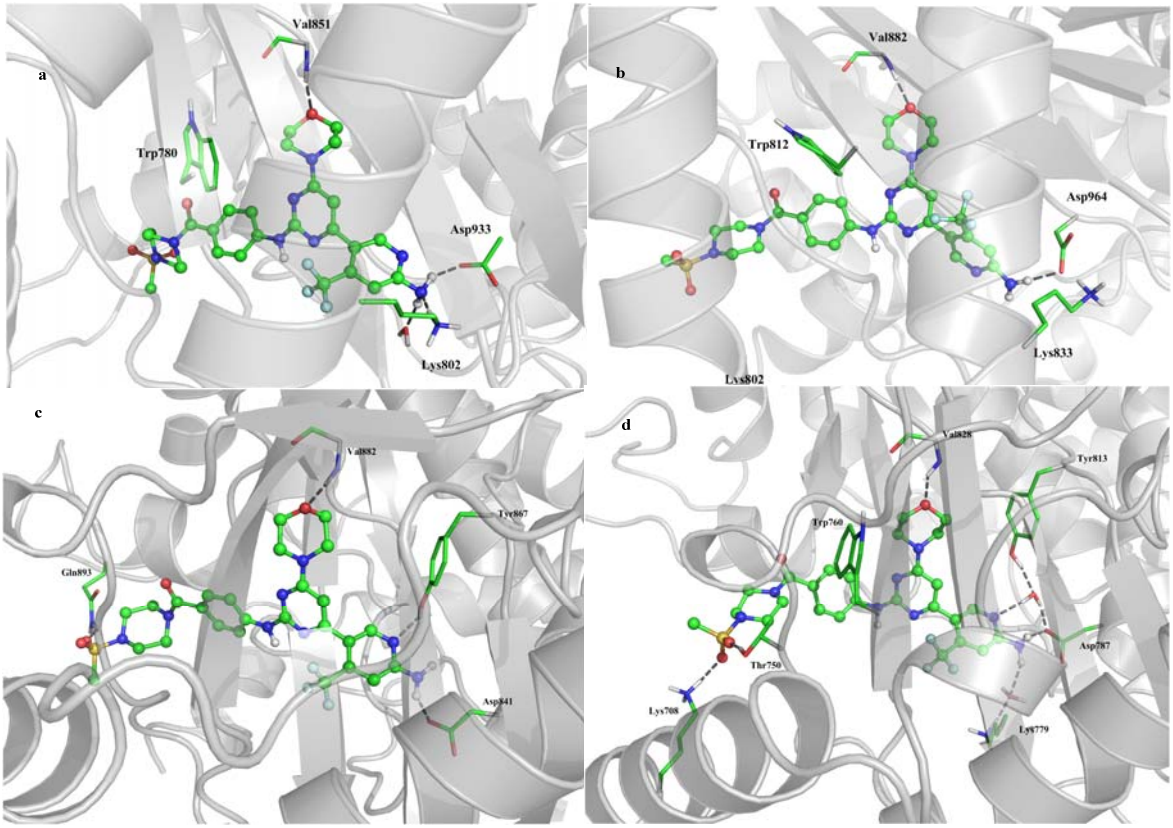

Scheme 1.

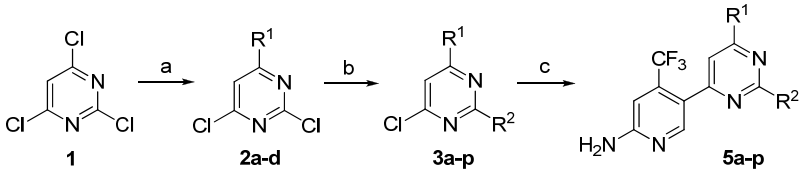

Scheme 2.

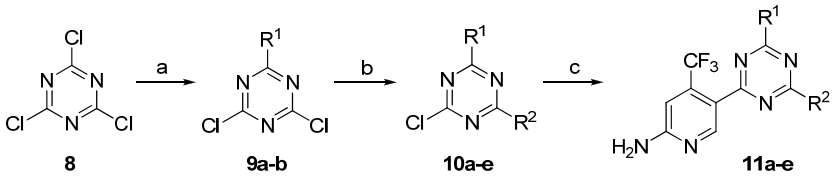

Scheme 3.

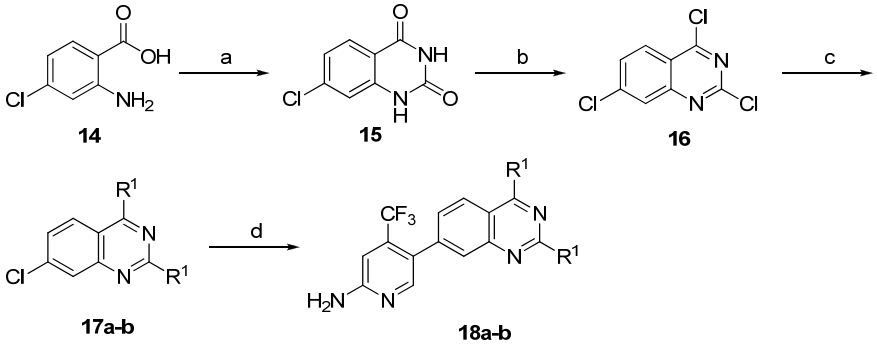

Scheme 4.

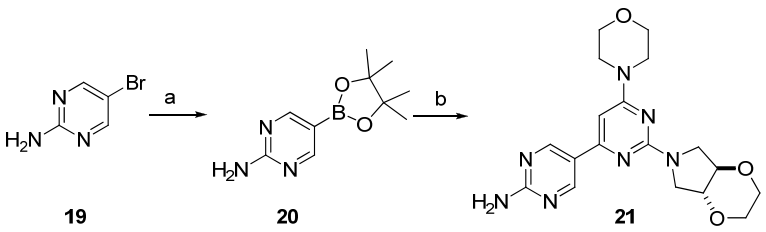

Scheme 5.

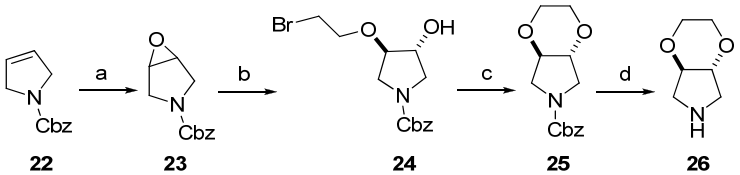

Table of contents graphic